

## Coating kinetics of fluoropolymer processing aids for sharkskin elimination: The role of droplet size<sup>☆</sup>

D. Bigio<sup>a</sup>, M.G. Meillon<sup>a</sup>, S.B. Kharchenko<sup>b</sup>, D. Morgan<sup>a</sup>, H. Zhou<sup>c</sup>,  
S.R. Oriani<sup>d</sup>, C.W. Macosko<sup>c</sup>, K.B. Migler<sup>b,\*</sup>

<sup>a</sup> University of Maryland, Department of Mechanical Engineering, College Park, MD, USA

<sup>b</sup> NIST, Polymers Division, Gaithersburg, MD, USA

<sup>c</sup> University of Minnesota, Department of Chemical Engineering & Material Science, Minneapolis, MN, USA

<sup>d</sup> DuPont Dow Elastomers L.L.C., Wilmington, DE, USA

Received 22 August 2004; received in revised form 1 April 2005; accepted 5 April 2005

### Abstract

The ability of fluoropolymer based polymer processing aids (PPA) to eliminate surface melt fracture (sharkskin) during extrusion of polyethylene is studied in relation to blend morphology (PPA droplet size) and processing conditions (shear rate). Under a constant throughput, the die entrance pressure, the PPA coating thickness and the degree of fracture are simultaneously monitored. The thickness of the fluoropolymer coating on the die surface is measured in situ through frustrated total internal reflection. A substantial enhancement in the coating rate and the magnitude of the steady state coating thickness as well as the faster elimination of sharkskin upon increase of PPA droplet size have been determined. These results are consistent with a recently developed model of the coating process.

© 2005 Elsevier B.V. All rights reserved.

**Keywords:** Sharkskin; Polyethylene; Extrusion; Blend; Domain size; Coating

### 1. Introduction

During the processing of polymers, flow instabilities often occur when certain critical conditions, such as viscosity and material throughput, are exceeded. These instabilities may limit equipment output, prevent new products from entering the market or force processors to accept materials with compromised quality. A major processing operation affected by flow instabilities is polymer extrusion, used in the manufacture of wires, sheets, tubes, films and other profiles.

For certain polymers, the following extrudate distortions can be observed as a function of increasing throughput: surface melt fracture (also known as sharkskin), stick-slip and gross melt fracture. Because sharkskin occurs at extrusion rates corresponding to typical polymer processing operations

and because it is the first instability to occur, there has been a sustained effort to understand and alleviate it. Sharkskin is characterized by a quasi-periodic roughness on the surface of the extrudate. Stick-slip occurs when pressure and flow rate oscillate causing the extrudate to have rough and smooth regions. During gross melt fracture, the extrudate distortions have a large amplitude chaotic appearance. Not all polymers show these three characteristic instabilities; a wide range of behavior has been reported. For summaries in this area, the reader is referred to recent reviews [1,2].

Sharkskin has been observed in polymers of high molecular mass and sufficiently narrow molecular mass distribution; it is readily observed in polyethylene (PE), such as high density PE and linear low-density PE as well as fluoropolymers, ethylene-propylene-diene monomer (EPDM) and polybutadiene and polydimethylsiloxane. This instability is generally undesirable because it causes a decrease in clarity and dimensional stability [3].

A great deal of effort has gone into unraveling the cause and cure of the sharkskin instability over the last two decades

<sup>☆</sup> Official contribution of the National Institute of Standards and Technology; not subject to copyright in the United States.

\* Corresponding author.

E-mail address: kalman.migler@nist.gov (K.B. Migler).

### Nomenclature

$A$	constant
$A'$	constant
$c$	concentration (mass/volume) of PPA in PPA/PE blend
$d$	average coating thickness
$l$	die length
$P$	pressure
$P_0$	pressure of pure PE
$Q_{in}$	mass in-flux
$Q_{out}$	mass out-flux
$R$	die radius
$S$	PPA particle radius
$t$	time
$t'$	non-dimensional time
$V_s$	slip velocity at PPA/PE interface
<i>Greek letters</i>	
$\dot{\gamma}_{PE}$	true shear rate of PE
$\dot{\gamma}_{PPA}$	true shear rate of PPA
$\dot{\gamma}_{PE}^a$	apparent shear rate of PE
$\dot{\gamma}_{PPA}^a$	apparent shear rate of PPA
$\rho$	mass density of PPA

[4–8]. For the purposes of the present work, we limit the discussion to a few relevant points. First, it has been established through several different methods that sharkskin originates at the exit of the die [9–12]. In particular, the material near the die exit undergoes strong extensional stresses [13], which rapidly accelerate and stretch the surface of the extrudate [14,15]. These stresses cause the polymer to fracture, a notion advanced by Cogswell [3], although the form of the fracture is not well understood. A related observation is that when the surface energy of the wall is reduced so that the polymer slips against the wall, the sharkskin is postponed to higher throughputs. For example, this occurs when a steel wall is replaced with the  $\alpha$ -brass [6,15]. Coating the die with a fluoropolymer such as polytetrafluoroethylene (PTFE) also leads to the elimination of sharkskin [16–19]. When slip occurs at the wall, the stresses on the polymer as it exits the die are greatly reduced which leads to the elimination of the instability [18,19].

Industrially, the most prevalent technique to modify the die surface for the extrusion of polyethylene (PE) involves incorporating a polymer processing aid (PPA) typically a fluoropolymer additive in low concentration (<0.1% by mass) [16,17]. Because the fluoropolymer is processable and immiscible in PE, it becomes distributed in the PE matrix in the form of discrete droplets. During the course of extrusion, these molten droplets come in contact with the die surface, where they adhere, and slowly flow towards the die exit. Once at the exit wall, the fluoropolymer layer eliminates sharkskin by allowing the PE to slip at the PE/fluoropolymer

interface. This is an industrially important example of polymer–polymer slippage, a subject that has been discussed theoretically [20,21] and realized experimentally with several different polymer pairs [18,22,23]. Because in the process of coating the die exit, the fluoropolymer also coats the full length of the die, use of a fluoropolymer PPA induces a reduction in pressure for a given throughput [16].

The crucial step in the action of the PPAs is the coating of the wall. Rosebaum et al. [24] have discussed the experimental observation that the time for complete coating of the surface of the die depends on shear rate, diameter and  $L/D$  of the die. The fluoropolymer coating has been observed to form streaks on the die wall in the direction of the flow [18,25–27]. Recently, it was shown that the appearance of the streaks roughly coincides with slippage of the PE and elimination of sharkskin [18,25]. Kharchenko et al. [25] developed an optical technique to carry out in situ measurement of the fluoropolymer coating thickness. They observed fluoropolymer deposition in streaks roughly 200 nm thick and several microns wide, depending on the processing conditions. They also showed that the fluoropolymer first coats the wall in the upstream contraction area of the die, followed by the downstream migration under stress. A semi-quantitative model to estimate the dependence of coating thickness on various parameters was developed.

Great potential for optimizing the use of PPAs exists because the vast majority of the fluoropolymer does not coat the wall; rather it is wasted by exiting in the bulk of the PE. Optimization of the coating process is highly desirable because it would allow PPAs to be used economically in more situations (as they have numerous secondary benefits such as reduced die-swell, die drool and gel build-up), and because it would allow end-users to utilize less PPA and reduce material costs. Thus, understanding the coating process is important, so that the parameters leading to improvements in coating efficiency can be exploited.

There is no clear evidence how the coating process may depend on the size of the particulates comprising the minor (PPA) phase. There is an indication in the literature that the PPA droplets smaller than 0.2  $\mu\text{m}$  would benefit the coating process [16], but there is also contrary evidence [28]. In this work, by applying an in situ optical reflectivity metrology and systematically tuning the PPA/PE morphology we were able to quantitatively verify the role of the PPA domain size on the coating kinetics.

In an effort to test a model of the coating process and to understand the factors that increase the coating efficiency, we quantify the effects of shear rate and fluoropolymer droplet size on the sharkskin elimination. We extrude blends with different PPA droplet sizes at several shear rates and measure the resulting coating thickness, the pressure reductions and the time for sharkskin elimination.

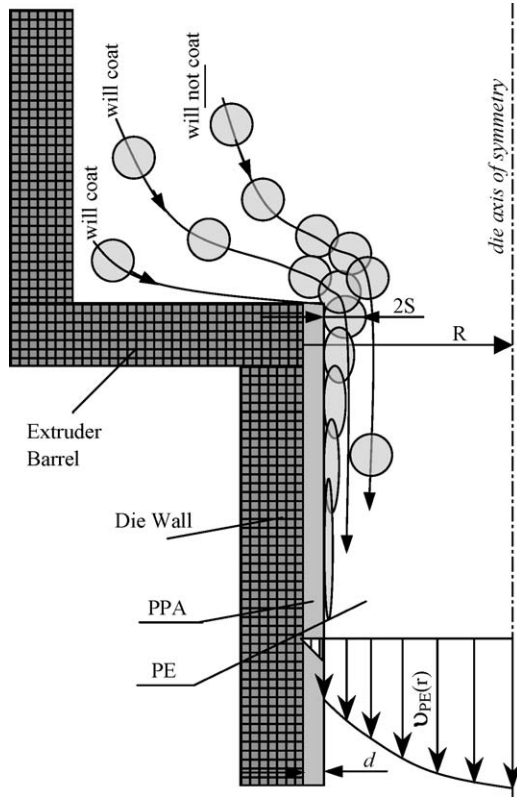


Fig. 1. Schematic of a PPA/PE flow in a circular die (from Kharchenko et al. [25]).

## 2. Deposition model

Related models describing the process whereby fluoropolymer droplets coat the die wall have been presented by Oriani and Chapman [28] and by Kharchenko et al. [25]. Both consider that the only droplets able to coat the wall are those whose natural streamlines take them sufficiently close (within one droplet radius to the wall). In the model by Kharchenko et al., droplets contact the entrance corner, flatten out into streaks as previously observed, and flow downstream due to the shear stress at the interface with the host polymer (see Fig. 1). Upon reaching the die exit, the fluoropolymer layer is gradually dragged out of the die where adhesive failure between the fluoropolymer and polyethylene causes most of the fluoropolymer to accumulate on external die surfaces, while a small amount of fluoropolymer remains on the surface of the extrudate [28]. In steady state, the in-flux from droplets coating the surface corner equals the out-flux from the fluoropolymer coating. Kharchenko et al. provide the expression for the flux of fluoropolymer depositing at the die entrance as

$$Q_{in} = 2\pi RSc \left( \frac{\dot{\gamma}_{PE} S}{2} + V_s \right) \quad (1)$$

where  $c$  is the concentration ( $\text{kg}/\text{m}^3$ ) of the polymer processing aid in the PPA/PE blend,  $V_s$  the PPA/PE interface slippage

velocity,  $S$  the radius of the PPA particle,  $\dot{\gamma}_{PE}$  the true shear rate of the PE at the PPA interface and  $R$  is the die radius. This model makes the assumption that the droplets that coat the wall have natural streamlines whose maximum separation from the corner is less than one droplet radius. Those droplets that do not contact the corner are subject to hydrodynamic forces that will move them further away from the wall [29,30]. For the out-flux from the die by the fluoropolymer which coated the wall, they find

$$Q_{out} = \pi d^2 R \rho \dot{\gamma}_{PPA} \quad (2)$$

where  $\rho$  is the mass density of the PPA and  $d$  is the average coating thickness. Under steady state conditions when the two fluxes are equal, we make the approximation ( $\dot{\gamma}_{PE} S/2 \ll V_s$ ). This is justified because Migler et al. found that  $V_s \approx 10 \text{ mm/s}$  under similar conditions [18], while  $\dot{\gamma}_{PE} S/2 \approx 0.3 \text{ mm/s}$  if one uses typical values of  $\dot{\gamma}_{PE} = 115 \text{ s}^{-1}$  and  $S = 5 \mu\text{m}$ . The thickness of the fluoropolymer layer is then given by

$$d = \left( \frac{2cV_s S}{\rho \dot{\gamma}_{PPA}} \right)^{\frac{1}{2}} \approx (2\rho c A' S)^{\frac{1}{2}} \quad (3)$$

where we have used the further approximation  $V_s \approx A \dot{\gamma}_{PE} \approx A' \dot{\gamma}_{PPA}$  [25] and  $A$  and  $A'$  are constants valid over the shear rates of interest. In this case  $A$  and  $A'$  are numerical constants reflecting the rough linearity of slippage data over a restricted range of shear rates, as observed in [18]. We note that this same relation holds for a thin rectangular die.

The above model predicts the steady state coating thickness, but also of great interest is the time it takes for a coating to develop from a die that is initially filled with the host PE. In a typical experiment, the extruder/capillary rheometer is first filled with the host polymer (PE), and the blend containing the PPA is subsequently introduced. Under these conditions, there is a finite time until sharkskin is relieved. The kinetics of the coating process is rather complex; we consider three stages in the process. In the first stage after the PPA blend is added to the extruder, the blend (containing the PPA as the minor component) first extrudes through the center of the die. It is far from the walls and there is no coating. As time progresses, the volume occupied by the blend increases, eventually filling most of the volume but leaving a small strip near the walls of pure PE. When the strip of pure material is of the same thickness as a typical PPA droplet, we anticipate that the larger droplets will be the first ones to be able to coat the wall. This is the second stage of the coating kinetics and Eq. (1) now becomes applicable. When the coating on the wall is sufficiently small that there is little slippage of the PE, then only the first term in parentheses of Eq. (1) is relevant

$$Q_{in} = \pi R S^2 c \dot{\gamma}_{PE} \quad (4)$$

as an approximation of the coating rate into the entrance corner of the die in Stage 2. Note the  $S^2$  dependence

of the deposition rate. In order for the sharkskin to be eliminated, the PPA must flow along the wall and be present at the exit lip. The third stage occurs as the coating builds up in the entrance corner causing the polyethylene to slip such that the second term in Eq. (1) dominates the first. This slippage greatly increases the PE velocity near the wall, which then allows more PPA to approach the wall per unit time. A real world complication to this picture is that the final coating is not uniform as mentioned previously, but rather has streaks in the direction of flow. A natural consequence of the model is that the disappearance of sharkskin does not occur uniformly along the extrudate but occurs in streaks, reflecting a streak-like nature of the coating process. Rather, it is autocatalytic, where the initial deposition in a particular spot enhances further deposition in the same place because of the increased flux due to slip. This has been observed experimentally by Kharchenko et al. in Fig. 7 (L2, L3) [25]. Therefore, PPAs coat the die in a streaky fashion. Thus, the coating thickness predictions reflect averages.

The duration of the second stage should be proportional to  $(Q_{in2})^{-1}$  because that parameter controls the time for sufficient coating to build up in order to cause slippage and enter into Stage 3. We can make an estimate of the time of Stage 3 by considering the time it takes to fully coat the die to a thickness of  $d$ . The total coating volume is  $V = 2\pi dRl$ , where  $l$  is the die length. The time required to coat the whole surface in Stage 3 is then

$$t = \frac{V}{Q_{in3}} = \frac{dl}{ScV_s} \sim \frac{dl}{ScA\dot{\gamma}_{PE}} \quad (5)$$

where we now assume that the slippage term (second term in parentheses) in Eq. (1) dominates the first.

The complexity of the coating process is such that an exact expression for the time to coat is not possible, but we can use the above discussion to make several testable predictions in regard to the coating rate and final thickness as a function of shear rate and droplet size. First, Eq. (3) indicates that the steady state thickness increases with the square root of droplet size. Second, Eq. (3) also predicts the final thickness should be independent of shear rate if the change in viscosity ratio of the two polymers is sufficiently small over the investigated shear rate range. Third, the time to achieve zero sharkskin scales as  $S^{-2}$  in Stage 2 and  $S^{-1}$  in Stage 3. Since the time for sharkskin elimination is one of the key metrics for the efficacy of a given PPA, this is quite relevant because it predicts that sharkskin should be eliminated much faster for larger droplets. Fourth, there is an inverse dependence on shear rate for the time scales of each stage (e.g. in Eq. (5) for Stage 3). The model thus predicts that for the same droplet size,  $t\dot{\gamma}$  is the invariant; the amount of material needed to be extruded in order to eliminate sharkskin will be the same as the shear rate is varied. We return to these predictions in Section 5.

### 3. Experimental

#### 3.1. Apparatus

We utilize the same apparatus as described by Kharchenko et al. [25] to measure the coating thickness. Because sharkskin melt fracture originates in the die exit region, we set out to measure the growth of the PPA coating about 2 mm from the exit of the die. Briefly, the apparatus consists of a circular sapphire die mounted on a capillary rheometer that has a square end at its the exit to simplify the acquisition of the optical signal. The frustrated total internal reflectance (Frustrated TIR) technique enables measurement of the thickness of the PPA coating on the die. The experiments were conducted at 180 °C using the die with a length  $l = 38.2$  mm and a radius  $R = 0.8$  mm.

#### 3.2. Materials

The carrier matrix used in this experiment was a linear low-density polyethylene (LLDPE LL1001.09 produced by Exxon-Mobil Company<sup>1</sup>, with density  $\rho = 918$  kg/m<sup>3</sup>, molecular mass  $M_w = 80$  kg/mol, melt index of 1 dg/min at 190 °C). The polymer processing additive, manufactured by DuPont Dow Elastomers, is a fluoroelastomer co-polymer of vinylidene fluoride and hexafluoropropylene in a 60/40 mass ratio with a specific gravity of 1.82. Supplied as pellets, the fluoroelastomer contains 0.7% barium sulfate as a dusting agent to prevent massing (pellets sticking together). Oscillatory rheological measurements of these materials shows that at the processing shear rates used in the present study the viscosities of the two polymers are approximately equal [25].

All experiments were conducted with a final blend of 0.1% by mass of the fluoropolymer. In order to obtain blends at this concentration with distinct droplet sizes, we employed the following procedure. Masterbatches containing 1 and 5% by mass of the fluoroelastomer in LLDPE were prepared by compounding on a 28 mm, three lobe, fully intermeshing twin-screw extruder, operating at a screw speed of 31 rad/s and a melt temperature of 200 °C. Altering the fluoroelastomer content of the blends provides a simple method of generating different size distributions of the PPA droplets in the continuous LLDPE phase as the more concentrated blend is subject to more coalescence during processing and results in a larger droplet size. These two PPA/LLDPE blends were further diluted to 0.1% PPA concentration using a Haake twin-screw extruder as described below. The 1% blend (containing the smallest fluoroelastomer droplets (2.3 μm, as described below) was subjected to the most intense melt mixing conditions (a screw speed of

<sup>1</sup> Certain equipment, instruments or materials are identified in this paper in order to adequately specify the experimental details. Such identification does not imply recommendation by the National Institute of Standards and Technology nor does it imply the materials are necessarily the best available for the purpose.

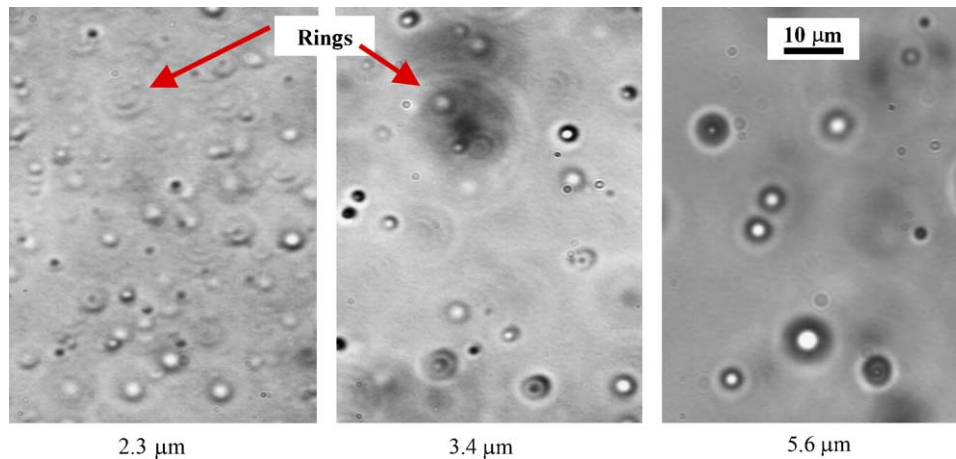


Fig. 2. Hot stage optical microscope images. Note the observed increase in size from left to right and the decrease in the number of particles from left to right. Faded rings represent out of focus particles. Notation defined from a weighted average.

7.23 rad/s and  $T=180^{\circ}\text{C}$ ) and the 5% blend that produced larger PPA droplets ( $3.4\ \mu\text{m}$ ), was extruded under ‘gentler’ conditions (1.36 rad/s and  $T=190^{\circ}\text{C}$ ). Finally, to obtain the 0.1% PPA/PE blend with the largest PPA droplets ( $5.6\ \mu\text{m}$ ), virgin fluoropolymer pellets were carefully dispersed in the PE matrix under the conditions of a very weak mixing flow (e.g., at a screw speed of 0.31 rad/s and  $T=220^{\circ}\text{C}$ ).

### 3.3. Image processing

Each 0.1% blend was analyzed to determine the domain size distribution of the fluoropolymer. The sample pellets were placed between two glass slides on a hot stage set to  $200^{\circ}\text{C}$  using an optical microscope with a  $100\times$  objective lens. Typical pictures of the three samples are shown in Fig. 2. The fluoropolymer appears as circular droplets in the polyethylene matrix. It can be observed that the diameter of the fluoropolymer droplets increases from the left picture to the right while, the number of particles decreases. There are certain parts of each picture where there are visible rings or

dim dark spots. These spots are particles that are out of focus and are not included in the domain size calculation.

To analyze the drop size, first the hot stage pictures were converted into density slice images using commercially available software (Fig. 3). Then the diameter of each highlighted particle was calculated. The results of the analysis are shown in Table 1. Also in this table are the calculated standard deviation, variance and the weighted diameter of each sample, which is used as the naming convention for the samples. The weighted diameter is an appropriate characterization of the droplet size distribution, because the development of a fluoropolymer coating on an extrusion die is a mass transfer phenomenon. As a result, a measure of the mass average for the fluoropolymer mass within the size distribution of droplets may be expected to be more useful than a measure based on how many particles of a particular size exist. In other words, although few large fluoropolymer droplets may exist in a given blend, just one of these large droplets may bring more mass to the die surface than dozens of smaller droplets. The normalized distribution of the recorded domain sizes is shown in Fig. 4.

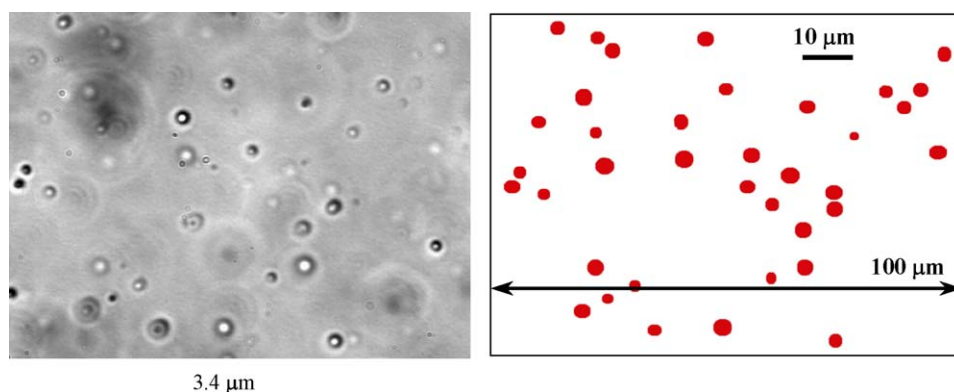


Fig. 3. Imaging density slice of the  $3.4\ \mu\text{m}$  sample. On the left is the original picture from the hot stage optical microscope and on the right is the density slice of the particles chosen.

Table 1  
Data calculated from domain size outputs of imaging

Initial concentration (by mass %)	Final concentration (by mass %)	Number average diameter ( $\mu\text{m}$ )	Standard deviation	Variance	Weight-average diameter ( $\Sigma d^4/\Sigma d^3$ )
1	0.1	2.0	0.4	0.2	2.3
5	0.1	2.9	0.7	0.5	3.4
Bulk	0.1	4.7	1.1	1.3	5.6

Sample size for each measurement is approximately 120 particles.

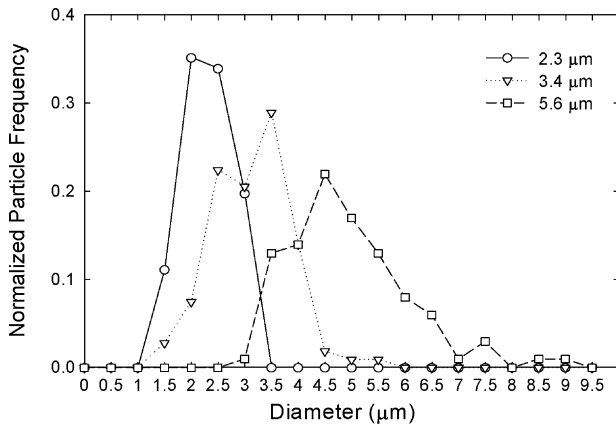


Fig. 4. Normalized distribution of the domain sizes for pre-extruded samples.

### 3.4. Procedure

First, pure LLDPE was extruded through the capillary rheometer to establish the entrance pressure drop and baseline optical reflectance readings. This control run also permitted observation of the extrudate surface appearance to ensure that fully developed sharkskin was present, thus confirming the absence of PPA. Next, the PPA/LLDPE blend under test was introduced while monitoring pressure near the die entrance, PPA coating thickness and extrudate appearance. Several loadings of 0.1% blend ( $\approx 20$  g each) were typically required to achieve steady state values in the entrance pressure and coating thickness. Experiments were conducted at a temperature of  $180^\circ\text{C}$  and apparent shear rates of 215, 155.5 and  $112.5\text{ s}^{-1}$ . The He–Ne laser intensities were collected in one spot on the die (2 mm upstream of the exit) between the loadings and these were used for the thickness measurements. At the conclusion of a test, the die was burned out at  $650^\circ\text{C}$  to remove any PPA residue before the next experiment. We also scraped and wiped clean the barrel.

## 4. Results

### 4.1. Effect of droplet size

Fig. 5 summarizes the reduction of the entrance pressure as a function of blend volume extruded for the three droplet sizes, at an apparent shear rate ( $\dot{\gamma}_{\text{PE}}^a$ ) of  $215\text{ s}^{-1}$ . The standard uncertainty in the pressure measurement was estimated

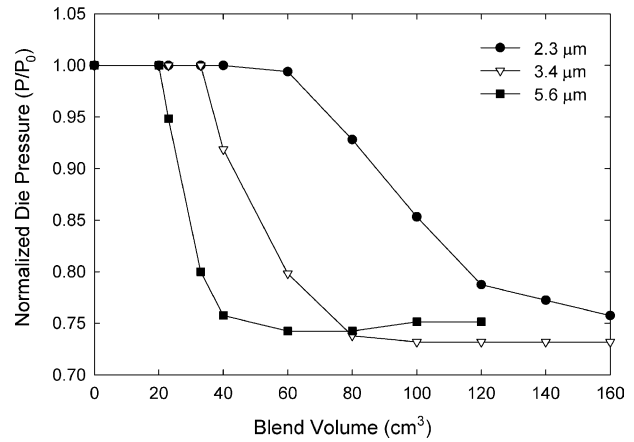


Fig. 5. Effect of the PPA domain size on the evolution of the normalized entrance pressure at  $\dot{\gamma}_{\text{PE}}^a = 215\text{ s}^{-1}$  as a function of extruded blend volume.

to be  $\pm 5\%$ <sup>2</sup> based on the pressure variation recorded during extrusion of several loads of pure LLDPE. The plots of pressure versus blend volume are normalized using the pressure readings for the pure PE. For all three droplet sizes, the extrusion pressure begins dropping even while the extrudate is completely melt fractured. This finding suggests that the fluoroelastomer coats regions of the die upstream of the exit before slowly co-extruding with the polyethylene to coat the die exit and eliminate melt fracture. In addition, the data in Fig. 5 shows that the rate of pressure reduction depends strongly on the fluoroelastomer droplet size entering the die, such that small droplets reduce the extrusion pressure more slowly than larger droplets. For example, the blend containing the smallest PPA domain size ( $2.3\text{ }\mu\text{m}$ ) was the least efficient in reduction of the pressure, requiring greater than  $40\text{ cm}^3$  of extrusion volume before a reduction in pressure is first observed and  $160\text{ cm}^3$  to reach a steady state pressure. In contrast, the mid-size blend ( $3.4\text{ }\mu\text{m}$ ) reached steady state after  $100\text{ cm}^3$ , whereas the blend with the biggest PPA domain size ( $5.6\text{ }\mu\text{m}$ ) required only about  $60\text{ cm}^3$  of extrusion volume to reach steady state. Taken together, these results imply that the *deposition rate at the die entrance* decreases with decreasing fluoroelastomer droplet size. For all three blends the steady state pressure values occurred at a similar reduction of about  $25 \pm 5\%$ . Also, we observed that sharkskin was eliminated at pressures slightly higher than the steady state ones, consistent with the earlier observations.

<sup>2</sup> Unless otherwise noted,  $\pm$  represents uncertainties of the measured values and refers to one standard deviation of the value.

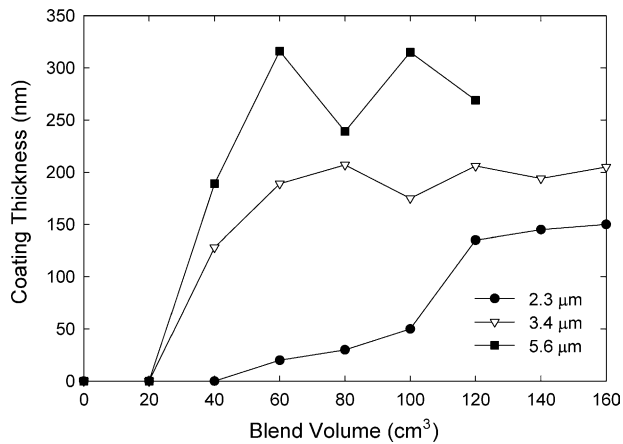


Fig. 6. Effect of the PPA domain size on the coating kinetics at  $\dot{\gamma}_{PE}^a = 215 \text{ s}^{-1}$ ; arrows mark a 0% melt fracture.

Fig. 6 shows the results of Frus-TIR measurements of the PPA coating thickness as a function of blend volume extruded and fluoroelastomer droplet size. In agreement with the pressure measurements, the blend with the smallest droplet size (2.3 μm) develops a fluoroelastomer die coating at the slowest rate. The coating first becomes optically detectable at 40 cm³ of extrusion volume, and reaches a final thickness of  $150 \pm 33 \text{ nm}$ . Both the mid-size blend (3.4 μm) and the blend with the largest droplets (5.6 μm) deposit a detectable coating after 20 cm³ of extrusion volume, but the midsize blend reaches a final thickness of  $200 \pm 34 \text{ nm}$ , whereas the coating from the large droplet blend grows faster and reaches a greater steady state thickness reached a  $315 \pm 120 \text{ nm}$ . The large droplet blend displays pronounced fluctuations in the coating thickness. The more finely dispersed blends show less time variation in coating thickness, possibly because the fluoropolymer layer at the die exit forms from a larger number of small droplets contacting the die surface.

Fig. 6 also shows the blend volume that passed through the die at the point when melt fracture was completely eliminated. As expected, based on the deposition rates discussed previously, a larger volume of the fluoroelastomer blend must be extruded to eliminate fracture as the fluoropolymer droplet size decreases. As a result, fluoropolymer blends containing small droplet sizes are markedly less effective in eliminating melt fracture than those containing larger droplets. The coating thickness at the point that fracture is eliminated, however, remains nearly constant regardless of droplet size, at about 150–180 nm. Thus, the improvement in PPA effectiveness as a result of increasing droplet size appears to be due solely to higher deposition rates on internal die surfaces, rather than to other phenomena not associated with slip at the polymer–die interface (e.g., slip between the fluoropolymer droplets and the polyethylene matrix).

Fig. 7 summarizes the reduction in the amount of sharkskin covering the surface of the extrudate as a function of blend volume passed through the die. The percent fracture is determined by visual inspection using a  $2.5\times$  objective

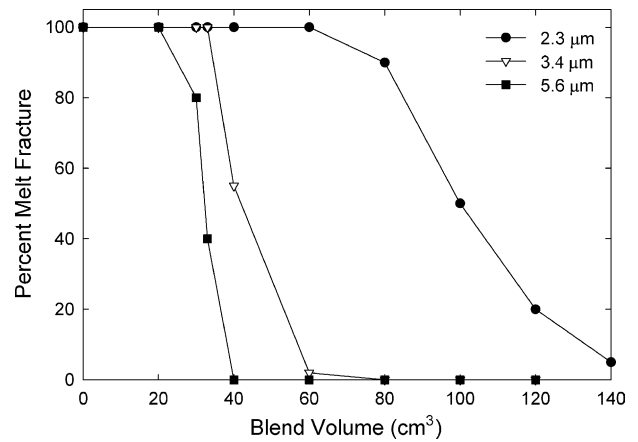


Fig. 7. Effect of the PPA domain size on the rate of sharkskin elimination at  $\dot{\gamma}_{PE}^a = 215 \text{ s}^{-1}$ .

lens, and error associated with this procedure is estimated to be  $\pm 5\%$ . The results in Figs. 5–7, when combined, clearly show that the growth of the fluoroelastomer layer on the die surface directly correlates with the rate of melt fracture elimination on the extrudate. Thus, the blend with the smallest PPA droplet size exhibits a significantly reduced rate of melt fracture elimination, compared to the blends containing larger PPA droplets.

#### 4.2. Effect of shear rate

The effect of the shear rate on the die coating process was investigated by running experiments using the 0.1% PPA/PE blend containing the largest PPA droplets (5.6 μm) at several apparent shear rates: 215, 155.5 and  $112.5 \text{ s}^{-1}$ . To normalize the data with respect to the total PPA input to the die as well as the pressure at the die entrance, Fig. 8 plots a reduced pressure ( $P/P_0$ ) as a function of blend volume passed through the die. For the three apparent shear rates, the pressure reduction starts at an approximately constant blend volume of 20 cm³. At steady state, the normalized pressure drop scales inversely

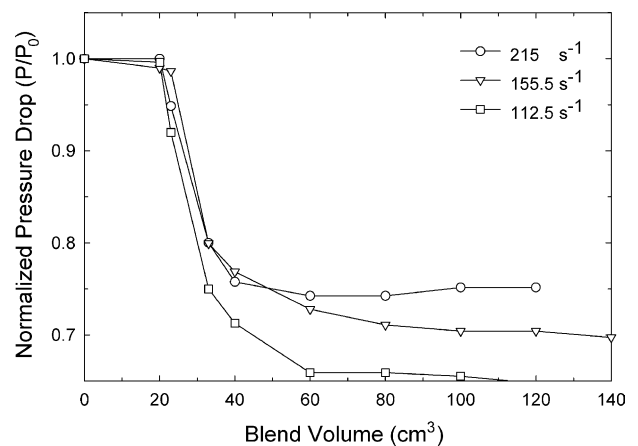


Fig. 8. Role of the apparent shear rate on the pressure drop during the extrusion of the 5.6 μm PPA/PE blend.

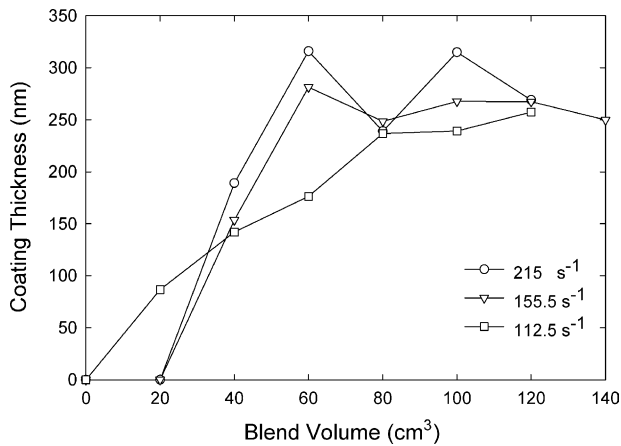


Fig. 9. Role of the apparent shear rate on the coating kinetics during the extrusion of the 5.6  $\mu\text{m}$  blend.

with the shear rate such that the 112.5  $\text{s}^{-1}$  run achieves a normalized pressure of 0.65, compared with 0.75 at an apparent shear rate of 215  $\text{s}^{-1}$ . These results are consistent with those of previous workers, where the shear stress differential between polymer flowing through a die with and without a PPA coating is a function of the shear rate [16].

The effect of the shear rate on the coating thickness is shown in Fig. 9. At the point when sharkskin melt fracture disappeared, the fluor elastomer coating thickness at the die exit ranged from 150 to 200 nm. Regardless of shear rate, the steady state coating thickness reached about 260 nm. The highest shear rate caused increasing fluctuations over time in the final coating thickness measurements, but the shear rate independence of the coating thickness is in agreement with the predictions from Eq. (3).

As follows from Fig. 10, the shear rate had no effect on the PPA effectiveness in eliminating sharkskin melt fracture when the data are presented as a function of extruded blend volume. Using the blend containing the largest PPA droplets, the quantity of blend required to reach 0% sharkskin remained constant for all three shear rates.

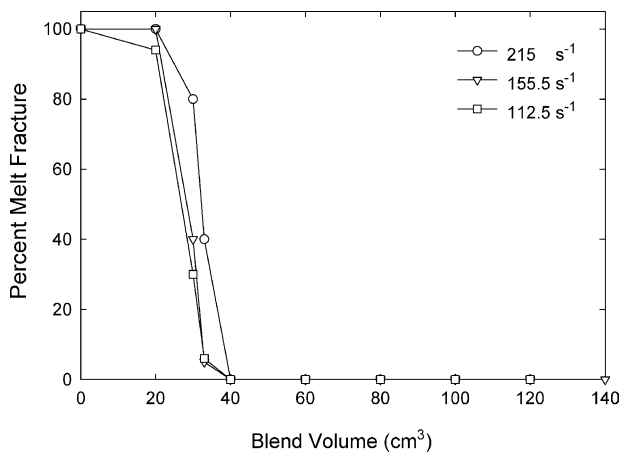


Fig. 10. Role of the apparent shear rate on the rate of sharkskin elimination during the extrusion of the 5.6  $\mu\text{m}$  blend.

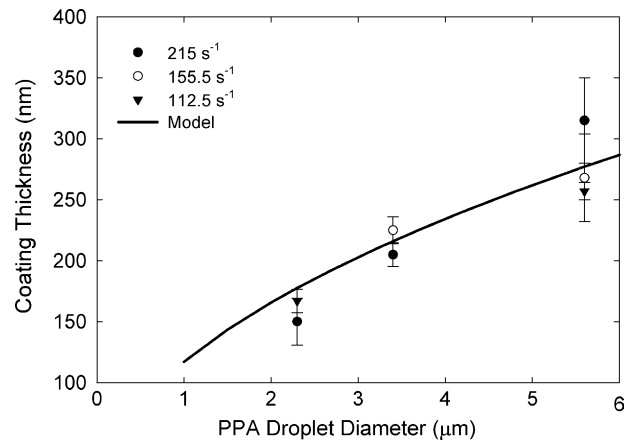


Fig. 11. Dependence of the steady state coating thickness on the PPA domain size. Experimental results are compared to model predictions (solid line) from Kharchenko et al. [25].

## 5. Discussion

We now compare the predictions made in Section 2 with our data, starting with the effect of shear rate on the coating process. From Fig. 9, we see that the steady state coating thickness is independent of apparent shear rate when the input drop size is constant, as predicted by Eq. (3). We find from Fig. 10 that for the same droplet size, the extruded blend volume required for the elimination of sharkskin is independent of shear rate (over the range investigated here). This result is consistent with the expectation of Section 2 where the model also predicts that the blends would start eliminating sharkskin at approximately the same blend volume (Fig. 10). One assumption in this model is that the droplet size does not change during the processing as the shear rate is increased. Preliminary data on droplet size of the extrudates does show that the droplet size distribution of the extrudate matches that of the resin that is fed into the capillary die. However, it is possible that in actual processing a screw-based extruder would create regions of high shear and would break up the droplets. This would lead to an increase in the extruded blend volume needed to eliminate sharkskin as the shear rate increases.

In terms of PPA droplet size, we can also compare our data to the predictions of Section 2. From Fig. 5, we see that the final die pressure is independent of droplet size, suggesting that the amount of slippage induced by the fluoropolymer is a function of shear stress and not coating thickness. We see from Fig. 6 that the steady state coating thickness is a function of droplet size. Eq. (3) predicts a square root dependence of coating thickness. Fig. 11 shows a plot of coating thickness versus droplet size; the solid curve is a fit of Eq. (3) where  $A'$  is the fitting parameter and we find  $A' = 0.028 \text{ mm}$ . Thus, the model clearly predicts the major trends in the data. Most importantly, as anticipated from the discussion on coating kinetics, we do observe the strong effect of PPA droplet size on the blend volume required to eliminate melt fracture (Fig. 7). In Fig. 12, the time to 0% melt

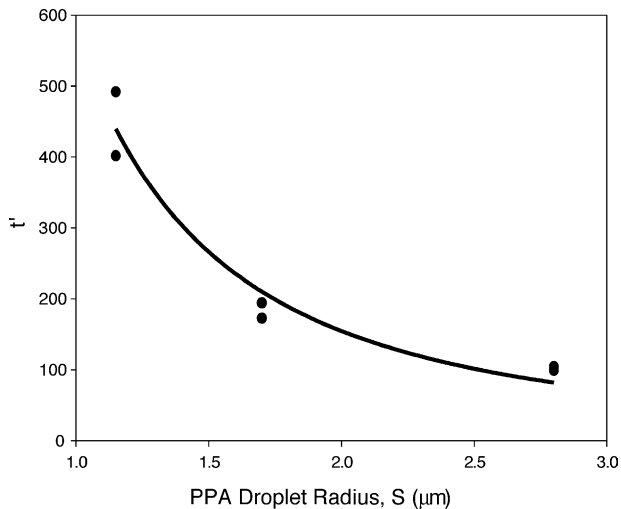


Fig. 12. Effect of PPA domain size on the non-dimensional time to 0% melt fracture  $t'$ . The solid line is a best fit power law with an exponent of  $-1.9$ .

fracture is plotted versus droplet size. The experimental time is non-dimensionalized with the shear rate and the PPA blend concentration ( $t' = t\dot{\gamma}c$ ). As predicted by Eq. (4), the plot reveals a power law dependence on  $S$  with a slope of nearly 2.

## 6. Conclusions

The extrusion of PPA/PE blends with known PPA droplet size elucidated the role of that size in the elimination of surface melt fracture. The parameters monitored were the reduction die entrance pressure, the coating thickness and the extrudate appearance. These measurements indicate that bigger particles establish thicker coatings and are more effective in eliminating melt fracture than smaller ones. Overall an entrance pressure reduction of about 70% was recorded when sharkskin was totally eliminated. Final coating thicknesses ranged from 150 to 300 nm with increasing PPA domain sizes. The amount of the PPA/PE blend with largest PPA droplets required to reach a smooth extrudate was about three to four times less compared to blends with the smaller PPA droplets. These results demonstrate that a productive way to enhance the efficiency of fluoroelastomer performance is to increase the droplet size. From the processing standpoint, there does not seem to be an upper limit on the most effective droplet size. However, if the droplets are too large, they could become defects in the finished extrudate.

## References

[1] M.M. Denn, Extrusion instabilities and wall slip, *Annu. Rev. Fluid Mech.* 33 (2001) 265–287.  
 [2] S.G. Hatzikiriakos, K.B. Migler, *Polymer Processing Instabilities: Control and Understanding*, Marcel Dekker, New York, 2004.

[3] F.N. Cogswell, Stretching flow instabilities at the exits of extrusion dies, *J. Non-Newtonian Fluid Mech.* 2 (1977) 37–47.  
 [4] N. El Kissi, J.M. Piau, F. Toussaint, Sharkskin and cracking of polymer melt extrudates, *J. Non-Newtonian Fluid Mech.* 68 (1997) 271–290.  
 [5] S.G. Hatzikiriakos, The onset of wall slip and sharkskin melt fracture in capillary-flow, *Polym. Eng. Sci.* 34 (1994) 1441–1449.  
 [6] A.V. Ramamurthy, Wall slip in viscous fluids and influence of materials of construction, *J. Rheol.* 30 (1986) 337–357.  
 [7] J. Perez-Gonzalez, M.M. Denn, Flow enhancement in the continuous extrusion of linear low-density polyethylene, *Ind. Eng. Chem. Res.* 40 (2001) 4309–4316.  
 [8] M.R. Mackley, R.P.G. Rutgers, D.G. Gilbert, Surface instabilities during the extrusion of linear low density polyethylene, *J. Non-Newtonian Fluid Mech.* 76 (1998) 281–297.  
 [9] R.H. Moynihan, D.G. Baird, R. Ramanathan, Additional observations on the surface melt fracture-behavior of linear low-density polyethylene, *J. Non-Newtonian Fluid Mech.* 36 (1990) 255–263.  
 [10] P.K. Dhoi, R.S. Jeyaseelan, A.J. Giacomini, J.C. Slattery, Common line motion III: implications in polymer extrusion, *J. Non-Newtonian Fluid Mech.* 71 (1997) 231–243.  
 [11] Y.W. Inn, R.J. Fischer, M.T. Shaw, Visual observation of development of sharkskin melt fracture in polybutadiene extrusion, *Rheol. Acta* 37 (1998) 573–582.  
 [12] G.V. Vinogradov, N.I. Insarova, B.B. Boiko, E.K. Borisenkova, Critical regimes of shear in linear polymers, *Polym. Eng. Sci.* 12 (1972) 323–334.  
 [13] R. Rutgers, M. Mackley, The correlation of experimental surface extrusion instabilities with numerically predicted exit surface stress concentrations and melt strength for linear low density polyethylene, *J. Rheol.* 44 (2000) 1319–1334.  
 [14] K.B. Migler, Y. Son, F. Qiao, K. Flynn, Extensional deformation, cohesive failure, and boundary conditions during sharkskin melt fracture, *J. Rheol.* 46 (2002) 383–400.  
 [15] T.J. Person, M.M. Denn, The effect of die materials and pressure-dependent slip on the extrusion of linear low-density polyethylene, *J. Rheol.* 41 (1997) 249–265.  
 [16] E.C. Achilleos, G. Georgiou, S.G. Hatzikiriakos, Role of processing aids in the extrusion of molten polymers, *J. Vinyl Addit. Technol.* 8 (2002) 7–24.  
 [17] S.E. Amos, G.M. Giacoletto, J.H. Horns, C. Lavallee, S.S. Woods, *Polymer Processing Aids (PPA)*, Hanser Gardner Publications Inc., Cincinnati, 2000.  
 [18] K.B. Migler, C. Lavallee, M.P. Dillon, S.S. Woods, C.L. Gettinger, Visualizing the elimination of sharkskin through fluoropolymer additives: coating and polymer–polymer slippage, *J. Rheol.* 45 (2001) 565–581.  
 [19] R.P.G. Rutgers, M.R. Mackley, The effect of channel geometry and wall boundary conditions on the formation of extrusion surface instabilities for LLDPE, *J. Non-Newtonian Fluid Mech.* 98 (2001) 185–199.  
 [20] F. Brochard-Wyart, P.G. Degennes, Sliding molecules at a polymer–polymer interface, *C.R. Acad. Sci., Ser. II* 317 (1993) 13–17.  
 [21] J.L. Goveas, G.H. Fredrickson, Apparent slip at a polymer–polymer interface, *Eur. Phys. J. B* 2 (1998) 79–92.  
 [22] Y.C. Lam, L. Jiang, C.Y. Yue, K.C. Tam, L. Li, Interfacial slip between polymer melts studied by confocal microscopy and rheological measurements, *J. Rheol.* 47 (2003) 795–807.  
 [23] R. Zhao, C.W. Macosko, Slip at polymer–polymer interfaces: rheological measurements on coextruded multilayers, *J. Rheol.* 46 (2002) 145–167.  
 [24] E. Rosebaum, S.G. Hatzikiriakos, C.W. Stewart, Flow implications in the processing of teflon, *Int. Polym. Proc. X* (1995) 204–212.  
 [25] S.B. Kharchenko, P.M. McGuiggan, K.B. Migler, Flow induced coating of fluoropolymer additives: development of frustrated

- total internal reflection imaging, *J. Rheol.* 47 (2003) 1523–1545.
- [26] C. Lavallée, Characterization of the polymer, processing additive (PPA) coating obtained on several extrusion dies, in: 2003 PLACE Conference and GLOBAL HOT MELT Symposium 2003, 2003.
- [27] S. Nam, Mechanism of fluoroelastomers processing aid in extrusion of LLDPE, *Polym. Process.* (1987) 98–101.
- [28] S.R. Oriani, G.R. Chapman, Fundamentals of melt fracture elimination using fluoropolymer process aids, *SPE ANTEC Technical Papers* 49, 2003, pp. 22–26.
- [29] M.R. Kennedy, C. Pozrikidis, R. Skalak, Motion and deformation of liquid drops, and the rheology of dilute emulsions in simple shear flow, *Comput. Fluids* 23 (1994) 251–278.
- [30] A. Karnis, S.F. Mason, Particle motions in sheared suspensions, *J. Colloid Interface Sci.* 24 (1967) 164–169.